Results and discussion. Mononuclear phagocytes in resident and induced populations present different stages of maturation but 2 extremes of cell morphology may be defined. The one corresponds to a small cell with relatively few surface processes and invaginations. It has few cytoplasmic granules and mitochondria and moderate amounts of rough ER. The other extreme is typified by a much larger cell with a more voluminous cytoplasm containing many organelles, abundant rough ER and a more extensive and irregular cell surface.

Large profiles in the resident sample accounted for only 43% of the total but the figure rises to some 72% after adjuvant challenge. This is taken to indicate that the resident population has relatively and absolutely fewer of the more mature cells since the largest cells must generate the largest profiles. Moreover, exposure to Freund's complete adjuvant evokes a florid peritoneal leucocytosis[13].

Morphometric differences between the 'average cell' in each (small and large) group are summarized in tables 1 and 2. Each value is an overall mean for 3 experiments. The data characterizing the total resident and induced populations are in very good agreement with earlier estimates[13].

The results suggest that cell maturation within a population involves the differential hypertrophy of all the compartments analyzed. Much of the increase in cell size (62% in resident, 65% in induced cells) results from expansion of the remaining cytoplasm which comprises free ribosomes, smooth ER, Golgi zones, phagosomes, centrioles and cytoplasmic ground substance. The rough ER contributes least (only 3–4%) to overall cell growth. The compartment which undergoes the greatest individual change is the granule: it increases by 141% in resident and by 205% in induced cells.

Mean organelle volumes were calculated from compartment volume and number. They reveal that the granule hypertrophy follows from increases in both number and size. In resident cells, the average granule is about 36% larger in 'large' cells (4.1×10^{-3} μm^3 versus 3.0×10^{-3} μm^3) and in induced cells the difference is even greater (10.6×10^{-3} μm^3 versus 4.8×10^{-3}). It would appear that number changes more than size in resident cells but the reverse obtains after adjuvant challenge and this may be an effect by certain adjuvant ingredients[13,14].

Expansion of the mitochondrial compartment is due solely to an increase in number since there is little, if any, change in size (mean volume about 5.5×10^{-2} μm^3). There was no evidence in the present model of any change in organelle length[4,11].

During maturation, cells acquire substantially more plasmalemma. Moreover, larger cells tend to have relatively more surface membrane than an equivalent sphere and are consequently less rounded[13] than smaller forms.

The overall picture of maturation given here validates earlier subjective impressions[4,9–12]. Smaller cells tend to have less plasmalemma, less rough ER, fewer granules and mitochondria. They therefore resemble more closely blood monocytes which typically have fewer surface features, reflecting their limited endocytic activity and membrane ruffling[4]. Differences in granule size may be determined by prior endocytosis and the fact that monocytes contain a peculiar type of granule not found in mature cells[6,16,17]. Changes in the amounts of ground cytoplasm and mitochondria may also reflect altered metabolic status and energy requirements[4].

Differences within a population are to be contrasted with those between resident and induced cells. Following adjuvant activation there is a considerable drop in mean granule content and a nett depletion of cell surface so that the average cell is rounder than normal[13,14]. Even those cells which are larger than the biggest cells in the resident fluid have, on average, fewer granules. However, they do have a more extensive surface. The affects of adjuvant probably result from the greater endocytic demands made on the cells, although the nature and degree of stimulation for resident cells are not yet clear.

1 I wish to thank Professor R. Barer for his advice and helpful criticism. Thanks are also due to the Wellcome Trust for financial support.

2 R.H. Ebert and H.W. Florey, Br. J. exp. Path. *20*, 342 (1939).
3 J.S. Sutton and L. Weiss, J. Cell Biol. *28*, 303 (1966).
4 Z.A. Cohn, Adv. Immun. *9*, 163 (1968).
5 B. Roser, J. reticuloendoth. Soc. *8*, 139 (1970).
6 R. van Furth, J.G. Hirsch and M.E. Fedorko, J. exp. Med. *132*, 794 (1970).
7 S. Gordon and Z.A. Cohn, Int. Rev. Cytol. *36*, 171 (1973).
8 R. van Furth and M.E. Fedorko, Lab. Invest. *34*, 440 (1976).
9 Z.A. Cohn, J.G. Hirsch and M.E. Fedorko, J. exp. Med. *123*, 747 (1966).
10 I. Carr, J. Path. Bact. *94*, 323 (1967).
11 D.F. Cappell, J. Path. Bact. *33*, 429 (1930).
12 A. Dumont, J. Ultrastruct. Res. *29*, 191 (1969).
13 T.M. Mayhew and M.A. Williams, Z. Zellforsch. mikrosk. Anat. *147*, 567 (1974).
14 T.M. Mayhew and M.A. Williams, Cell Tissue Res. *150*, 529 (1974).
15 E.R. Weibel, Int. Rev. Cytol. *26*, 235 (1969).
16 B.A. Nichols, D.F. Bainton and M.G. Farquhar, J. Cell Biol. *50*, 498 (1971).
17 B.A. Nichols and D.F. Bainton, Lab. Invest. *29*, 27 (1973).

Asialoprotein uptake by liver cells: Immunofluorescence microscopy[1]

A.V. LeBouton and G. Lippman

Department of Anatomy, College of Medicine, University of Arizona, Tucson (Arizona 85724, USA), 3 July 1978

Summary. Uptake of asialoproteins by hepatocytes causes a change in the intracellular pattern of immunofluorescence. Control cells display a peripheral fluorescence which probably represents nascent proteins. Dark nonfluorescent areas, that presumably contain glycogen, are located around the nucleus. In contrast, liver cells from rats injected with asialoproteins display a pancytoplasmic fluorescence due to an influx of endocytotic vesicles.

A concept is currently emerging that certain highly metabolic organs, such as the liver, extend their influence within the body via interaction with mobile carrier structures such as plasma proteins[2–5]. The idea is exemplified by current studies on interactions between liver cells and certain glycoproteins that have had their terminal sialic acid residue removed (asialoproteins). Thus, asialo-ceruloplasmin[6], alpha-1 acid glycoprotein[7], interferon[8], fibrinogen[9] and alpha-1 antitrypsin[10] are rapidly cleared from the circulation and sequestered in the liver.

Additional biochemical findings show that hepatocytes are the target cells; receptors specific for asialoproteins have

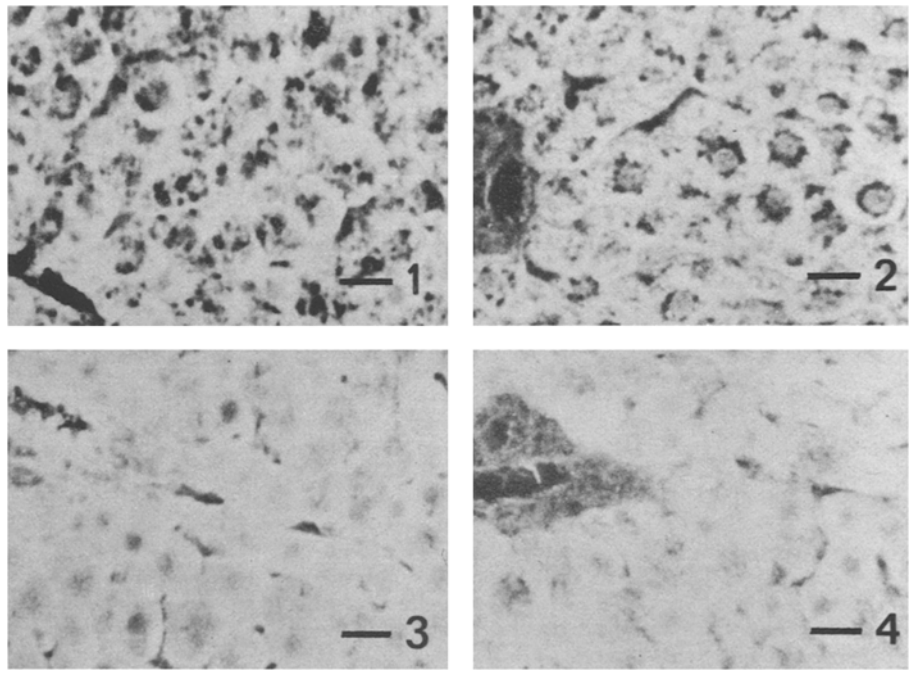

Fig. 1–4. Immunofluorescent detection of serum globulins in liver cells. Small portal areas are to the left (× 500). Figure 1: from control rat injected with saline. Figure 2: from control rat injected with normal serum. In both cases specific fluorescence appears peripherally within hepatocytes; nonglobulin-containing areas are centrally located around the nucleus. Figure 3: from experimental rat injected with acid-hydrolyzed serum proteins. Figure 4: from experimental rat injected with neuraminidase-treated serum proteins. In both cases specific fluorescence is spread evenly across the hepatocytes. The solid bar represents 20 µm.

been found on the plasma membrane of liver cells[11-15]. What is lacking, however, is definitive morphological evidence to show how many hepatocytes engulf asialoproteins. Such information is necessary if the magnitude of the liver's role in this important process is to be assessed. Accordingly, morphologic analyses have been done by using radioautography after injection of ^{3}H-asialoproteins[6,7]. In such cases the injected radioactivity was small and the biopsy specimen was fixed in a formaldehyde solution. These conditions can create a problem, however, because it has been shown that during formalin-fixation of blood-filled liver specimens, plasma proteins leak into hepatocytes[16]. If not taken into account, this artifact could lead to the erroneous conclusion that the presence of radioisotopically tagged asialoprotein in liver cells was due entirely to active uptake, whereas it may be due, at least in part, to passive diffusion of the labeled protein into cells prior to fixation.

Therefore, to obtain a more accurate image of asialoprotein uptake by liver cells we injected rats with asialoproteins and prepared liver specimens for immunofluorescence microscopy under newly developed conditions known to prevent passive diffusion of proteins into cells. This approach clearly demonstrates with confidence, that hepatocytes are capable of actively internalizing asialoserum proteins.

Lyophilized samples of normal rat serum were desialyated by either acid hydrolysis[14] or neuraminidase treatment[17]. The extent of sialic acid release was estimated with the thiobarbituric acid method[18]. A standard dilution curve was prepared with N-acetylneuraminic acid (Sigma). The amount of sialic acid released compared to that calculated to be present originally[19] was 73% after acid hydrolysis and 91% after neuraminidase treatment. Samples from both treatments were extensively dialyzed in the cold against phosphate buffered saline, lyophilized and reconstituted with distilled water just before use.

Asialoserum (or intact serum) was injected i.v. into male Sprague-Dawley rats (0.137 mg/g b.wt, average b.wt 425 g) between 08.00 h and 09.00 h. The animals were killed 20 min later, immediately after being heparinized (50 units i.v.). They were then exsanguinated from the inferior vena cava through a needle and syringe. The portal vein was cannulated and the liver flushed free of blood with 50 ml of normal saline containing 0.04% sodium nitrite at 37 °C. The liver was dissected out, placed in ice-cold saline and cut into slices 1.5 mm thick in a Stadie-Riggs microtome. A sharpened brass cork borer (4.5 mm diameter) was then used to punch out wafers from the slices. The liver wafers were rapidly fixed at room temperature for 30 min in 1% acetic acid in 95% ethanol under constant agitation with a magnetic stirrer[20]. Paraffin sections (6 µm) were then prepared, with time in the various reagents held to a minimum.

The presence of asialoserum proteins was demonstrated with the indirect fluorescent antibody method[21]. The primary antiserum was rabbit anti-rat total serum globulins and the secondary was goat anti-rabbit gamma globulin conjugated with fluorescein isothicyanate (Cappel Labs). In the controls, the primary antiserum was absorbed with excess rat serum, or only the secondary antiserum was used. Both types of control were negative.

The fixative used is similar in composition to Rossman's or Carnoy's fluids (ethanolic solutions of a weak acid), which are known to offer good cytological preservation of glycogen. Therefore, we interpret the dark globulin-negative areas in hepatocytes from the 2 controls as concentrations of glycogen particles (figures 1 and 2). Since all rats were killed at the same time of day, they should all have been in nearly identical nutritional states. Thus we assume that glycogen was also present in liver cells from the experimental animals but was scattered by the large influx of endocytotic vesicles containing asialoproteins[22] (figures 3 and 4). A similar phenomenon has been seen in uptake of fluorescein labeled phytohemagglutinin by leucocytes, where the specific granules in eosinophils were displaced by fluorescent endocytotic vesicles[23].

Biochemical evidence has shown that unlike other asialoproteins, asialotransferrin is not internalized by liver cells[3]. Accordingly, we analyzed some of our experimental specimens for transferrin content and found that in all cases they appeared identical to controls, corroborating the non-hepatic uptake of asialotransferrin.

1 We thank Prof. J.B. Angevine, C.W. Kischer and B. Magun for criticizing earlier drafts of this manuscript. Supported by the Arizona Foundation and USPHS grant SO7RRO5675.
2 P.J. Winterburn and C.F. Phelps, Nature, Lond. *236,* 147 (1972).
3 G. Ashwell and A.G. Morell, Adv. Enzymol. *41,* 99 (1974).
4 V. Bocci, Experientia *32,* 135 (1976).
5 J.F. Dice and A.L. Goldberg, Nature, Lond. *262,* 514 (1976).
6 A.G. Morell, R.A. Irvine, I. Sternlieb and I.H. Scheinberg, J. biol. Chem. *243,* 155 (1968).
7 P.P. van Rijk and C.J.A. van den Hamer, J. Lab. clin. Med. *88,* 142 (1976).
8 V. Bocci, A. Pacini, G.P. Pessina, V. Bargigli and M. Russi, Experientia *33,* 164 (1977).
9 J. Martinex, J. Palascak and C. Peters, J. Lab. clin. Med. *89,* 367 (1977).
10 S.D. Yu and J.C. Gan, Arch. Biochem. Biophys. *179,* 477 (1977).
11 W.E. Pricer, Jr, and G. Ashwell, J. biol. Chem. *246* (1971).
12 T. Kawasaki and G. Ashwell, J. biol. Chem. *251,* 5292 (1976).
13 W.E. Pricer, Jr, and G. Ashwell, J. biol. Chem. *251,* 7539 (1976).
14 R.J. Stockert, A.G. Morell and I.H. Scheinberg, Biochem. biophys. Res. Commun. *68,* 988 (1976).
15 R.J. Stockert, A.G. Morell and I.H. Scheinberg, Science *197,* 667 (1977).
16 A.V. LeBouton, Anat. Rec. *190,* 457 (abstr.) (1978).
17 E. Regoeczi, M.W.C. Hatton and K.L. Wong, Can. J. Biochem. *52,* 155 (1974).
18 L. Warren, J. biol. Chem. *234,* 1971 (1959).
19 R.L. Engen, A. Anderson and L.L. Rouze, Clin. Chem. *20,* 1125 (1974).
20 M. Horikawa, N. Chisaka, S. Yokoyama and T. Onoe, J. Histochem. Cytochem. *24,* 926 (1976).
21 M. Goldman, Fluorescent Antibody Methods, p. 157. Academic Press, New York 1968.
22 G. Gregoriadis, A.G. Morell, I. Sternlieb and I.H. Scheinberg, J. biol. Chem. *245,* 5833 (1970).
23 L. Razavi, Nature, Lond. *210,* 444 (1966).

Frequency and distribution of tubulo-filamentous nuclear inclusions in the celiac ganglion of the cat as revealed by serial sections

J. Vuillet-Luciani, M. Vio, C. Cataldo and R. Seïte[1]

Laboratoire d'Histologie I, Groupe de Neurocytobiologie, Faculté de Médecine, F-13385 Marseille Cédex 4 (France), 7 July 1978

Summary. On sections at random of a cat celiac ganglion we counted 68 sections of nuclear inclusions (NI) for 320 sections of neuronal nuclei, i.e. an 'apparent' frequency of 0.20. As revealed by serial sections the 'actual' frequency is higher since the 5 nuclei entirely explored exhibit 19 NI. Such a study shows that each nucleus may contain at least 3 and up to 5 different tubulo-filamentous NI.

We have previously shown that the nuclei of sympathetic neurons in stellate, superior-cervical and celiac ganglia of the cat contain inclusions similar to the so-called intranuclear rodlets of the light microscopy. These nuclear inclusions (NI) consisting of filaments and/or tubules can be classified in 5 principal types, namely: filamentous spindle-shaped inclusions (type I), tubular spindle-shaped inclusions (type II), tubulo-filamentous spindle-shaped inclusions (type III), crystalloid inclusions formed only by filaments (type IV), crystalloid inclusions composed by filaments and tubules (type V)[2-4].

One of the most important problems dealing with these nuclear structures is to know whether they are common or uncommon, i.e. to fix their frequency of occurrence according to species and loci. In the sympathetic ganglia of the cat we have shown that these inclusions are encountered in all adult animals studied, with variations in frequency of occurrence from animal to animal. This frequency has been shown strongly increased following electrical stimulation[5] or local perfusion of cAMP analogs and theophylline in treated stellate ganglia compared to controlled ones[6]. These results suggest that filaments and tubules are normal components of the nucleus of sympathetic neurons and reflect the level of neuronal activity[2,6]. This frequency has been fixed by counting the number of sections of NI in 320 sections of neuronal nuclei on tissue sections taken at random in the ganglia, named in this work 'apparent' frequency. The 'apparent' frequency varies from 0.008 to 0.20 in the controlled ganglia[5,6].

The problem is to know which is the actual distribution of the NI for a given 'apparent' frequency, otherwise to know whether the phenomenon occurs in the whole neuronal population or only in some neurons of sympathetic ganglia. Such an answer should be found in a statistical processing of the quantitative data as far as the volume and size of these inclusions could be identified to a simple geometric pattern. So that it is the distribution of the nuclear bodies taken as spheres could be determined by some authors[7].

Cell	Type I Filamentous spindle-shaped inclusions	Type II Tubular spindle-shaped inclusions	Type III Tubulo-filamentous spindle-shaped inclusions	Total number of inclusions by neuron
A	4	1	0	5
B	2	1	0	3
C	3	1	0	4
D	3	1	0	4
E	2	0	1	3
Total number of inclusions	14	4	1	
Percentage (serial sections)	74	21	5	
Percentage (sections at random)	59	15	24	